HNUE JOURNAL OF SCIENCE DOI: 10.18173/2354-1059.2022-0026
Natural Sciences 2022, Volume 67, Issue 2, pp. 94-102
This paper is available online at http://stdb.hnue.edu.vn

INVESTIGATION OF I-V CHARACTERISTICS OF CARBON NANOTUBES AND TIN OXIDE NANOWIRES HETEROJUNCTION FOR GAS SENSING APPLICATIONS

Quan Thi Minh Nguyet[1], Tran Thi Ngoc Hoa[2], Nguyen Van Duy[3], Nguyen Duc Hoa[3] and Nguyen Van Hieu[4]

[1]School of Engineering Physics, Hanoi University of Science and Technology
[2]Department of Medical Physics, Hanoi Medical University
[3]International Training Institute for Materials Science, Hanoi University of Science and Technology
[4]Faculty of Electrical & Electronic Engineering, Phenikaa University

Abstract. In this study, heterojunctions of carbon nanotubes (CNTs) and tin oxide nanowires (SnO_2) were investigated to determine their electrical performance for gas sensing applications. The I–V characteristics of the heterojunction were measured in air and H_2S gas. The electrical parameters such as barrier height ϕ_B, ideality factor n, series resistance R_s, and reverse saturation current I_o were extracted from the I-V plots. In H_2S gas, the barrier height ϕ_B and series resistance R_s are lower compared to air, whereas the ideality factor n and saturation current I_o are higher. These findings are essential for promoting technologies aimed at forming high-quality heterojunctions for gas sensing applications.

Keywords: Heterojunction, carbon nanotubes, SnO_2 nanowires, gas sensing.

1. Introduction

Heterojunctions are the technological keys to many electronic and optoelectronic devices. In recent decades, low-dimensional nanostructures of many materials have been successfully fabricated. Nano heterojunctions have also been studied to improve the gas sensing characteristics [1]. The potential barrier height of these heterojunctions is very sensitive to external agents. Especially at the nanoscale, where the material is very porous, gases are easily absorbed and drastically change the potential barrier height of the junction. This makes the sensor more sensitive [2-4]. Following this trend, heterojunctions of individual materials such as semiconductor metal oxide nanowires (SMO-NWs) [5], CNTs [6], Graphene (GP) [7], transition metal Dichalcogenides (TMDs) [8] were investigated for application in new sensor generations. Due to many

Received June 14, 2022. Revised June 23, 2022. Accepted June 30, 2022
Contact Quan Thi Minh Nguyet, email address: nguyet.quanthiminh@hust.edu.vn

interesting properties, the heterojunctions of metal oxides semiconductor nanowires and CNTs are attracting interest in applied research in a wide range of electronic components [9], including diodes or supercapacitors on flexible substrates [10-14], electrochemical devices [15], and field emission [16]. Carbon nanomaterials can exhibit p-type semiconductor or metallic properties depending on the structure [17] so the junctions between carbon nanomaterials and metal-semiconductor oxides can be p-n or Schottky. Such heterojunctions are not only fundamentally attractive from the perspective of electronic devices but also very promising for sensing applications. Research by Dai et al. showed that the heterojunction between nano-bar α-Fe_2O_3 and CNTs was highly sensitive to acetone gas and the detection limit reached 500 ppb concentration [18]. Another study by Lupan et al. [19] showed that transitions between ZnO nanowires and CNTs could detect NH_3 gas at room temperature with a detection limit of 400 ppb. Research by Li et al. [20] showed the ability of NO_2 gas sensitivity at room temperature of the sensor based on the transition between ZnO nanowires and m-SWCNTs metal electrodes. The response of the ZnO/m-SWCNTs structure to 2.5 ppm NO_2 at room temperature reached about 52%. Recently, we successfully fabricated the SnO_2/CNTs heterojunctions for NO_2 gas sensing applications [21-23], the results show that these heterojunctions have potential applications in highly sensitive gas sensors. However, the gas sensing mechanisms of these structures have not been clarified. Therefore, understanding the fundamental physical and electrical properties of the SnO_2/CNTs heterojunction is important for the development of applications based on this structure.

To explain the sensing mechanism of the gas sensors based on heterojunction structures, most studies have suggested that the change in barrier height at the contact between the two materials plays an important role in the sensitivity of the gas [24, 25]. In this study, the I-V characteristics of CNTs/SnO_2 were investigated in different gas environments to determine the heterojunction characteristics such as saturation leakage current, ideal factor, barrier height, and series resistance to elucidate the gas sensing mechanism.

2. Contents

2.1. Experiments

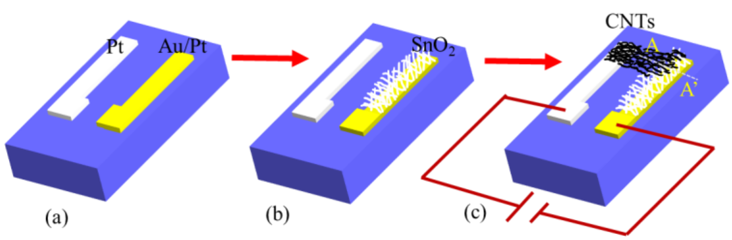

Figure 1. Scheme for fabrication of the heterojunction: (a) Pt and Au-catalyzed Pt electrodes, (b) selective growth of SnO_2 nanowires, and (c) CNTs/SnO_2 heterojunction

The heterojunctions CNTs/SnO_2 are fabricated on electrodes with the structure as shown in Figure 1. First, the sensor chip with one Pt electrode and one Au-catalyzed Pt electrode (Figure 1(a)) is fabricated by conventional photolithography and sputtering methods. SnO_2 nanowires were fabricated directly on an Au-catalyzed Pt electrode (Figure 1(b)) by the thermal vapor deposition method [26]. The gap between the two electrodes is designed to be wide enough and the technological parameters in the fabrication process are controlled such that the SnO_2 nanowires are dense enough to completely cover the electrode but not long enough to bridge the two electrodes [22]. In detail, high purity tin powders (99.9%, Sigma Aldrich) were used as the reaction source. For growing nanowires, 0.1 g of tin powders were loaded in an alumina boat, which was then placed inside the center of a horizontal quartz tube furnace. The distance between the electrodes and the alumina boat was about 2 cm. The whole system was evacuated to a pressure of 1.5×10^{-1} Torr using a rotary pump and then purged with high purity argon. Then the furnace was heated up to 750 ^oC for 20 mins from room temperature and maintained for 15 mins under a flow of oxygen at 0.5 sccm. Finally, the system was cooled down naturally to room temperature. In this study, the commercial CNTs with diameters of about 60-100 nm were dispersed in an aqueous solvent and surfactant P123. After fabrication of SnO_2 nanowires, CNTs were coated onto the electrode by dip-coating to form CNTs/SnO_2 heterojunctions (Figure 1(c)). The complete device was annealed at 350 ^oC for 2 hours to remove solvents.

The characteristics of the CNTs/SnO_2 heterojunctions have been investigated by FE-SEM methods (JEOL 7600F) and Raman (Micro-Raman InVia, RENISHAW, H44840, Laser 633 nm). The I-V characteristics of the junctions were investigated at different temperatures, voltages, and gas conditions using a Keithley 2602 source and controlled by the Labview program. To measure the I-V characteristic, the CNTs/SnO_2 heterojunction is biased by applying DC voltage to the two electrodes which are shown in Figure 1c. The junction is forward biased by connecting CNTs to the positive terminal, the SnO_2 nanowires to the negative terminal of the power supply, and vice versa in the case of reverse bias.

2.2. Results and discussion

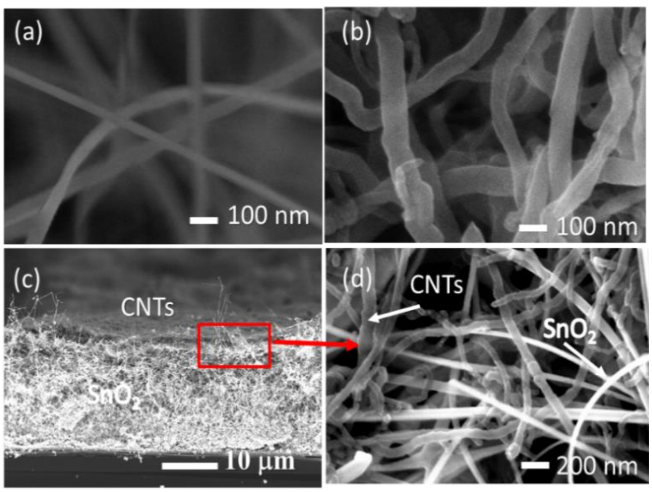

Figure 2. (a) SnO_2 nanowires grown directly on a Pt electrode, (b)The commercial CNTs diameter d:60-100 nm. (c) The cross-section SEM image of the CNTs/SnO_2 heterojunctions, (d) enlarged image of the CNTs randomly networked on top of SnO_2 nanowires

The morphology of SnO_2 nanowires, the commercial CNTs, and CNTs/SnO_2 heterojunction were observed by SEM and the results are presented in Figure 2. SEM image of SnO_2 directly grown on Pt electrode by the thermal vapor deposition method in Figure 2 (a) shows that the diameter of the nanowires is about 40-60 nm. The high-magnification SEM image in Figure 2 (b) revealed that CNTs with a diameter of 60-100 nm are uniformly dispersed and have high porosity. The SEM image of A-A'cross-section (Figure 1(c)) of the heterojunction was presented in Figure 2c, which can be seen in the high density SnO_2 nanowires completely covering the Pt electrode and CNTs form a film on top of SnO_2. The enlarged image in Figure 3 (d) shows that the CNTs randomly networked come into contact with on-chip grown SnO_2 nanowires at the junction area.

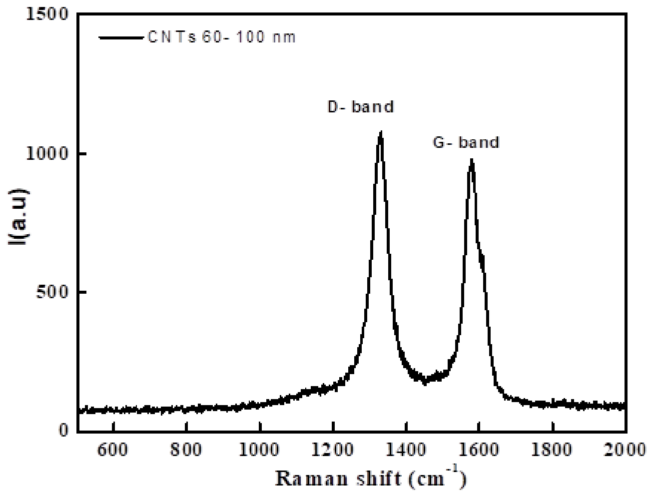

Figure 3. Raman spectra were taken on SnO_2/CNTs heterojunctions

The Raman spectra of the heterojunctions are presented in Figure 3. The spectrum reveals two main typical modes of MWCNTs: the D band at 1342 cm^{-1}, which is activated by the presence of disorder in carbon systems, and the G band at 1580 cm^{-1}, which is assigned to the in-plane vibration of the C–C.

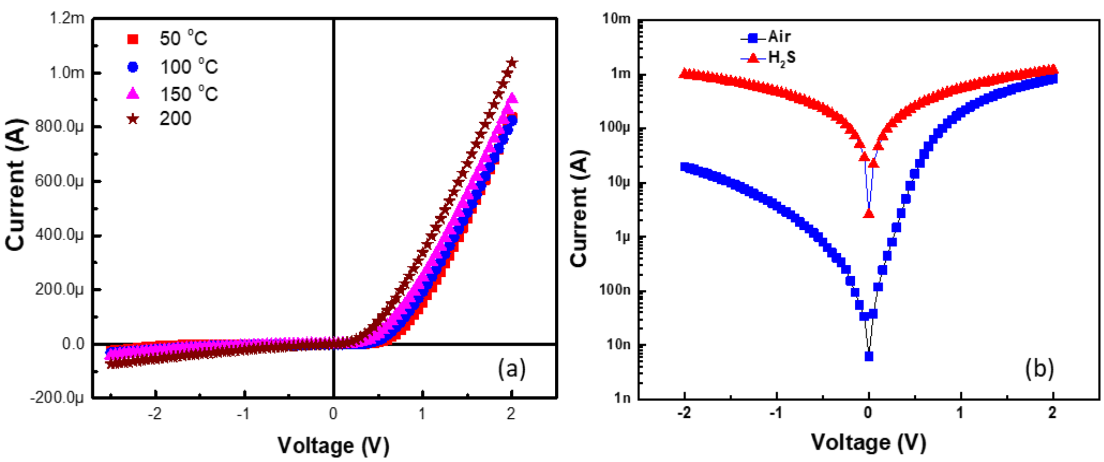

Figure 4. (a) I-V plot of CNTs/SnO_2 heterojunction in the air at different temperatures, (b) I-V plots of CNTs/SnO_2 heterojunction in air and 0.25 ppm H_2S at 100 °C

The I-V characteristics of the CNTs/SnO_2 heterojunctions in the air at the temperatures of 50 °C, 100 °C, 150 °C, and 200 °C are presented in Figure 4 (a). It can be seen that, in the bias voltage range from -2 V to +2 V, the CNTs/SnO_2 heterojunctions exhibit good rectification at operating temperatures from 50 °C to 200 °C. Since the contacts between SnO_2 and CNTs with the Pt electrode are Ohmic [21], the rectification property of the structure is due to the formation of a potential barrier at the junction between the SnO_2 nanowires and CNTs. It also proves that the CNTs network is only in contact with the left Pt electrode and in contact with the SnO_2 nanowires that have grown directly on the right Pt electrode (as shown in Figure 1 (c)). The I-V characteristics of the CNTs/SnO_2 heterojunction were studied at 100 °C in an H_2S gas concentration of 0.25 ppm. The results in Figure 4 (b) show that in H_2S gas, the current through the junction is increased compared to in the air. The variation of leakage current in analytical gas is larger than in forward-biased current. At a bias voltage of -2 V, the leakage current in the air has a value of about 20 μA in H_2S 0.25 ppm the leakage current increased to 1 mA.

The CNTs/SnO_2 heterojunction can be described using the equivalent circuit model shown in Figure 5. The diode component in the circuit represents the interface between CNTs and SnO_2. R_{CNTs} and R_{SnO2} are series resistance of CNTs and SnO_2. From the I-V characteristics, the diode parameters of the equivalent circuit model including saturation leakage current, ideality factor, potential barrier height, and series resistance of the junction can be calculated.

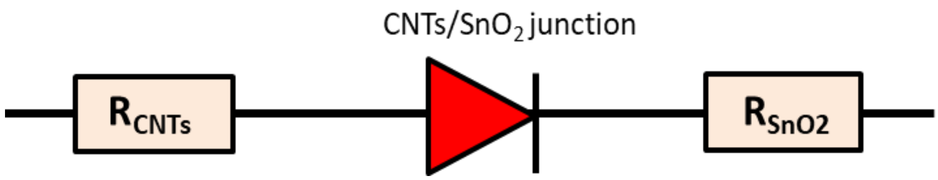

Figure 5. Equivalent circuit model of the CNTs/SnO_2 heterojunctions

According to many studies, the relationship between the current and the voltage of the nano-heterojunction can be described according to the thermal emission theory (TE) model [3, 27, 28]. For bias voltage $V > 3k_BT/q$, the relation between the applied forward bias and current can be calculated by the following equation:

$$I = I_o \exp\left(\frac{qV}{nk_BT}\right) \tag{1}$$

where

$$I_o = AA^*T^2 \exp\left(\frac{-q\phi_B}{k_BT}\right) \tag{2}$$

where I_o *(A)* is the saturation current, n is the ideality factor, k_B *(J/K)* is Boltzmann constant, q *(C)* is the electron charge, T *(K)* is absolute temperature, A *(cm²)* is the area of the junction estimated by the area of the electrode, A^* *($Acm^{-2}K^{-2}$)* is effective Richardson constant, and ϕ_B *(eV)* is the barrier height of the heterojunction.

Taking the natural logarithm of (1) we have

$$lnI = lnI_o + \frac{qV}{nk_BT} \tag{3}$$

The linear fitting on the *lnI* vs. *V* plots of the heterojunction in the linear region of experimental data in air and 0.25 pp H_2S gas at a temperature of 100 ^oC was presented in Figure 6. We determined the values of *n* and I_o from the slope and the y-axis intercept of the fitted straight line.

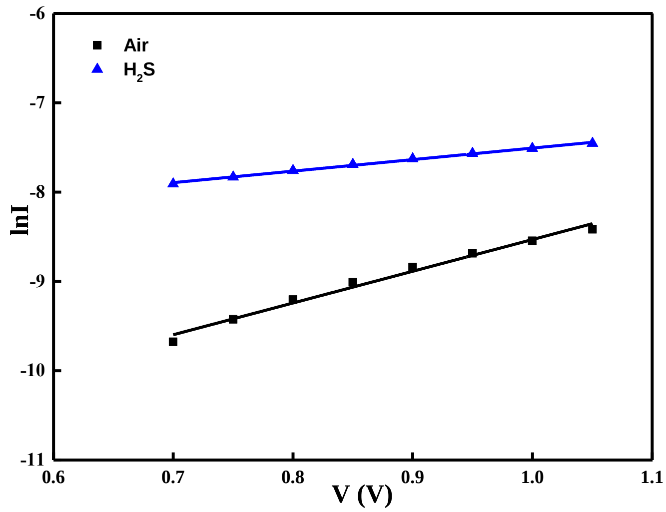

Figure 6. lnI-V plot of the CNTs/SnO$_2$ heterojunction in Air and 0.25 ppm H$_2$S at a temperature of 100 ^oC

If we consider the effect of series resistance R_s caused by CNTs and SnO_2, equation (1) becomes

$$I = I_o \exp\left(\frac{q(V - IR_s)}{nk_BT}\right) \tag{4}$$

The forward bias current-voltage characteristics due to thermionic emission of the heterojunction with series resistance can be expressed as Cheung's functions [29, 30].

$$\frac{dV}{d(lnI)} = IR_s + \frac{nk_BT}{q} \tag{5}$$

$$H(I) = V - \left(\frac{nk_BT}{q}\right)\ln\left(\frac{I}{AA^*T^2}\right) \tag{6}$$

$$H(I) = IR_s + n\phi_B \tag{7}$$

In Figure 7(a-b), the intercept and slope of the line can be determined by linearly fitting the graph of equation (5) *dV/d(lnI)* vs. *I*. *H(I)* is defined from (6) using the value of n and the data of *I-V* characteristics. The slope and y-axis intercept of the linear fitting of Plotting *H(I)* vs. *I* should give the heterojunction barrier height.

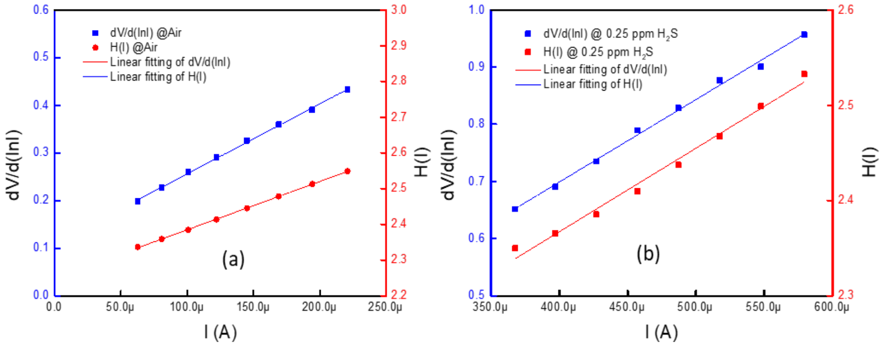

Figure 7.** **The dV/d(lnI)** **vs.** **I and H(I)** **vs.** **I plots of the CNTs/SnO₂ heterojunction in the air (a) and 0.25 ppm H₂S at a temperature of 100 °C

The parameters of the CNTs/SnO_2 heterojunction were calculated based on the I-V characteristics and are presented in Table 1. It was observed that values of I_o, n, R_s, and ϕ_B are all changed in the analytical gas environment. In H_2S gas, the barrier height ϕ_B and series resistance R_s are decreased compared to in air while ideality factor n and saturation current I_o increased. The barrier height is observed to decrease from 0.66 eV in the air to 0.53 eV in 0.25 ppm H_2S. The saturation current I_o increased from $5.65.10^{-6}$ A in the air to $1.51.10^{-4}$ A in 0.25 ppm H_2S. Alternatively, a rise in the ideality factor in H_2S gas suggests a reduction in the rectification behavior of the heterojunction. In addition, the series resistance does not change appreciably, which shows that the gas sensitivity mechanism is dictated by the contact between CNTs and SnO_2 nanowires.

Table 1. Parameters obtained from I-V characteristics of CNTs/SnO₂ heterojunction in Air and 0.25 ppm H₂S

Parameters	Air	0.25 ppm H_2S
I_o (A)	$5.65.10^{-6}$	$1.51.10^{-4}$
n	3.4	3.8
R_s (Ω)	1466	878
ϕ_B (eV)	0.66	0.53

3. Conclusions

In summary, the CNTs/SnO_2 heterojunctions have been successfully fabricated which exhibit good rectification at operating temperatures from 50 °C to 200 °C. An equivalent circuit model of the junction was proposed and the diode parameters including the ideality factor, the barrier height, and the series resistance were extracted based on the thermionic emission theory from I−V measurements in air and H_2S gas. As a result, the barrier height decreased from 0.66 eV in the air to 0.53 eV in 0.25 ppm H_2S. The saturation current I_o increased from $5.65.10^{-6}$ A in the air to $1.51.10^{-4}$ A in 0.25 ppm H_2S. The ideality factor in H_2S is higher than in the air. However, the series resistance in H_2S does not change significantly compared to in the air. These results are of great importance for assisting the development of technologies aimed at forming high-quality heterojunctions for gas sensing applications.

Acknowledgment. This research was financially supported by the Vietnam Ministry of Education and Training under project No. B2020-BKA-26-CTVL.

REFERENCES

[1] D. R. Miller, S. A. Akbar, and P. A. Morris, 2014. Nanoscale metal oxide-based heterojunctions for gas sensing: A review. *Sensors Actuators, B Chem.*, Vol. 204, pp. 250-272.

[2] R. T. Tung, 2014. The physics and chemistry of the Schottky barrier height. *Appl. Phys. Rev.*, Vol. 011304.

[3] Y. Hu, J. Zhou, P. H. Yeh, Z. Li, T. Y. Wei, and Z. L. Wang, 2010. Supersensitive, fast-response nanowire sensors by using Schottky contacts. *Adv. Mater.*, Vol. 22, No. 30, pp. 3327-3332.

[4] J. Yu, S. J. Ippolito, W. Wlodarski, M. Strano, and K. Kalantar-zadeh, 2010. Nanorod based Schottky contact gas sensors in reversed bias condition. *Nanotechnology*, Vol. 21, No. 26, 265502.

[5] D. Chen *et al.*, 2022. High sensitive room temperature NO_2 gas sensor based on the avalanche breakdown induced by Schottky junction in TiO_2-Sn_3O_4 nano heterojunctions. *J. Alloys Compd.*, Vol. 912, No. 2, 165079.

[6] Y. Zhao *et al.*, 2018. Outstanding gas-sensing performance of CuO-CNTs nanocomposite based on asymmetrical Schottky junctions. *Appl. Surf. Sci.*, Vol. 428, pp. 415-421.

[7] A. Bag, D. Bin Moon, K. H. Park, C. Y. Cho, and N. E. Lee, 2019. Room-temperature-operated fast and reversible vertical-heterostructure-diode gas sensor composed of reduced graphene oxide and AlGaN/GaN. *Sensors Actuators, B Chem.*, Vol. 296, No. March, 126684.

[8] A. Shokri and N. Salami, 2016. Gas sensor based on MoS_2 monolayer. *Sensors Actuators, B Chem.*, Vol. 236, pp. 378-385.

[9] J. G. Ok, S. H. Tawfick, K. A. Juggernauth, K. Sun, Y. Zhang, and A. J. Hart, 2010. Electrically addressable hybrid architectures of zinc oxide nanowires grown on aligned carbon nanotubes. *Adv. Funct. Mater.*, Vol. 20, No. 15, pp. 2470-2480.

[10] J. Yoon, K. W. Min, J. Kim, G. T. Kim, and J. S. Ha, 2012, P-*n* hetero-junction /diode arrays of *p*-type single-walled carbon nanotubes and aligned *n*-type SnO_2 nanowires. *Nanotechnology*, Vol. 23, No. 26, 265301.

[11] J. Park, Y. Kim, G. T. Kim, and J. S. Ha. 2011. Facile fabrication of SWCNT/SnO_2 nanowire heterojunction devices on a flexible polyimide substrate. *Adv. Funct. Mater.*, Vol. 21, No. 21, pp. 4159-4165.

[12] P. C. Chen, G. Shen, S. Sukcharoenchoke, and C. Zhou, 2009. Flexible and transparent supercapacitor based on In_2O_3 nanowire/carbon nanotube heterogeneous films. *Appl. Phys. Lett.*, Vol. 94, No. 4, pp. 2007-2010.

[13] S. D. Perera *et al.*, 2011. Vanadium oxide nanowire-carbon nanotube binder-free flexible electrodes for supercapacitors. *Adv. Energy Mater.*, Vol. 1, No. 5, pp. 936-945.

[14] A. S. Al-Asadi *et al.*, 2017. Aligned carbon nanotube/zinc oxide nanowire hybrids as high-performance electrodes for supercapacitor applications. *J. Appl. Phys.*, Vol. 121, 124303.

[15] G. Q. Mo, J. S. Ye, and W. De Zhang, 2009. Unusual electrochemical response of ZnO nanowires-decorated multiwalled carbon nanotubes. *Electrochim. Acta*, Vol. 55, No. 2, pp. 511-515.

[16] X. Yan, B. K. Tay, and P. Miele, 2008. Field emission from ordered carbon nanotube-ZnO heterojunction arrays. *Carbon N. Y.*, Vol. 46, No. 5, pp. 753-758.
[17] R. A. Bell, 2015. *Conduction in Carbon Nanotube Networks*. Springer International Publishing Switzerland.
[18] M. Dai *et al.*, 2017. Hierarchical Assembly of α-Fe_2O_3 Nanorods on Multiwall Carbon Nanotubes as a High-Performance Sensing Material for Gas Sensors. *ACS Appl. Mater. Interfaces*, Vol. 9, No. 10, pp. 8919-8928.
[19] O. Lupan, F. Schütt, V. Postica, D. Smazna, Y. K. Mishra, and R. Adelung, 2017. Sensing performances of pure and hybridized carbon nanotubes-ZnO nanowire networks: A detailed study. *Sci. Rep.*, Vol. 7, No. 1, pp. 1-12.
[20] X. Li, J. Wang, D. Xie, J. Xu, Y. Xia, and L. Xiang, 2017. Enhanced p-type NO_2-sensing properties of ZnO nanowires utilizing CNTs electrode. *Mater. Lett.*, Vol. 206, pp. 18-21.
[21] Q. T. Minh Nguyet *et al.*, 2017. Superior enhancement of NO_2 gas response using n-p-n transition of carbon nanotubes/SnO_2 nanowires heterojunctions. *Sensors Actuators, B Chem.*, Vol. 238, No. 2, pp. 1120-1127.
[22] Q. T. M. Nguyet, N. Van Duy, C. Manh Hung, N. D. Hoa, and N. Van Hieu, 2018. Ultrasensitive NO_2 gas sensors using hybrid heterojunctions of multi-walled carbon nanotubes and on-chip grew SnO_2 nanowires. *Appl. Phys. Lett.*, Vol. 112, No. 15, pp. 1-6.
[23] Quan Thi Minh Nguyet, Nguyen Van Duy, Chu Manh Hung, Nguyen Van Hieu, 2017. In-situ fabrication of SnO_2 nanowires/carbon nanotubes heterojunctions based NO_2 gas sensors. *J. Sci. Technol.*, Vol. 118, pp. 036-039.
[24] T. Wei, P. Yeh, S. Lu, and Z. L. Wang, 2009. Gigantic Enhancement in Sensitivity Using Schottky Contacted Nanowire Nanosensor. *J. Am. Chem. Soc.* Vol. 131, No. 22, pp. 17690-17695.
[25] M. Zhang, L. L. Brooks, N. Chartuprayoon, W. Bosze, Y. Choa, and N. V. Myung, 2013. Palladium/Single-Walled Carbon Nanotube Back-to-back Schottky Contact-based Hydrogen Sensors and Their Sensing Mechanism. *Appl. Mater. Interfaces*, Vol. 6, pp. 319-326.
[26] V. T. Duoc, C. M. Hung, H. Nguyen, N. Van Duy, N. Van Hieu, and N. D. Hoa, 2021. Room temperature highly toxic NO_2 gas sensors based on rootstock/scion nanowires of SnO_2/ZnO, ZnO/SnO_2, SnO_2/SnO_2, and ZnO/ZnO. *Sensors Actuators B Chem.*, Vol. 348, No. 2.
[27] Y. Ling, F. Ren, and J. Feng, 2016. Reverse bias voltage-dependent hydrogen sensing properties on Au e TiO_2 nanotubes Schottky barrier diodes. *Int. J. Hydrogen Energy*, Vol. 41, No. 18, pp. 2-9.
[28] H. Aydin *et al.*, 2018. Experimental and computational investigation of graphene/SAMs/n-Si Schottky diodes. *Appl. Surf. Sci.*, Vol. 428, pp. 1010-1017.
[29] S. K. Cheung and N. W. Cheung, 1986. Extraction of Schottky diode parameters from forward current-voltage characteristics. *Appl. Phys. Lett.*, Vol. 49, No. 2, pp. 85-87.
[30] C. Yim, N. McEvoy, H.-Y. Kim, E. Rezvani, and G. S. Duesberg, 2013. Investigation of the Interfaces in Schottky Diodes Using Equivalent Circuit Models. *ACS Appl. Mater. Interfaces*, Vol. 5, No. 15, pp. 6951-6958.